Acid-Catalyzed Breakdown of Alkoxide and Thiolate Ion Adducts of Benzylidene Meldrum's Acid, Methoxybenzylidene Meldrum's Acid and Thiomethoxybenzylidene Meldrum's Acid

Claude F. Bernasconi,*[,†] Rodney J. Ketner,[†] Shoshana D. Brown,[†] Xin Chen,[‡] and Zvi Rappoport[‡]

Department of Chemistry and Biochemistry, University of California, Santa Cruz, California 95064, and Department of Organic Chemistry, The Hebrew University of Jerusalem, Jerusalem 91904, Israel

Received June 29, 1999

A kinetic study of the acid-catalyzed loss of alkoxide and thiolate ions from alkoxide and thiolate ion adducts, respectively, of benzylidene Meldrum's acid (**1-H**), methoxybenzylidene Meldrum's acid (**1-OMe**), and thiomethoxybenzylidene Meldrum's acid (**1-SMe**) is reported. The reactions appear to be subject to general acid catalysis, although the catalytic effect of buffers is weak and the bulk of the reported data refers to H^+-catalysis. α-Carbon protonation and, in some cases, protonation of one of the carbonyl oxygens to form an enol compete with alkoxide or thiolate ion expulsion. This rendered the kinetic analysis more complex but allowed the determination of pK_a values and of proton-transfer rate constants at the α-carbon. In conjunction with previously reported data on the nucleophilic addition of alkoxide and thiolate ions to the same Meldrum's acid derivatives, rate constants for nucleophilic addition by the respective neutral alcohols and thiols could also be calculated. Various structure−reactivity relationships are discussed that help define transition-state structures. Comparisons with similar reactions of alkoxide ion adducts of *β*-alkoxy-α-nitrostilbenes provide additional insights.

Introduction

We have been engaged in a research program aimed at improving our understanding of structure−reactivity relationships in nucleophilic vinylic substitution reactions (S_NV)[1] that proceed by the addition−elimination mechanism. Our focus has been on reactions where the intermediate accumulates to detectable levels and allows a direct kinetic determination of the individual steps in the mechanism.[2] In such systems much more can be learned about the factors that determine reactivity than is possible when the intermediate remains at steady-state levels.

Recent examples are the reactions of methoxybenzylidene Meldrum's acid, **1-OMe**,[3] and thiomethoxybenzylidene Meldrum's acid **1-SMe**,[4] with alkoxide and thiolate ion nucleophiles. The mechanistic scheme is

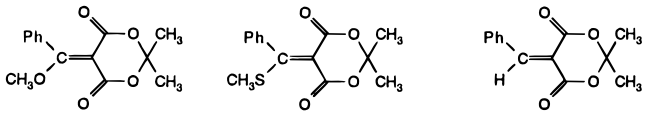

1-OMe **1-SMe** **1-H**

illustrated in eq 1 for the reaction of **1-OMe** with a

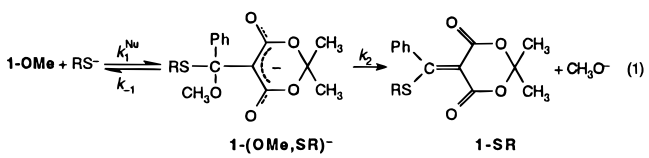

1-(OMe,SR)⁻ **1-SR** (1)

thiolate ion.

One aspect of these reactions which has not received much attention is the *acid-catalyzed* breakdown of the intermediate, either toward products or toward reactants. These processes are shown in eq 2 for the **1-OMe**/RSH

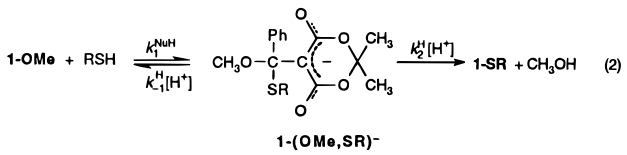

1-(OMe,SR)⁻ (2)

system; note that in this case the microscopic reverse of the H^+-catalyzed breakdown of the intermediate toward reactants is solvent-assisted nucleophilic attack by the protonated nucleophile. The possibility of buffer catalysis will be brought up later.

The processes shown in eq 2 can be studied in experiments where the intermediate is first generated by the reaction of the vinylic substrate with the anionic nucleophile ($Nu^- = RS^-$ in this case) in basic solution and then

† University of California.
‡ The Hebrew University.

(1) For reviews, see (a) Rappoport, Z. *Adv. Phys. Org. Chem.* **1969**, *7*, 1. (b) Modena, G. *Acc. Chem. Res.* **1971**, *4*, 73. (c) Miller, S. I. *Tetrahedron* **1977**, *33*, 1211. (d) Rappoport, Z. *Acc. Chem. Res.* **1981**, *14*, 7. (e) Rappoport, Z. *Recl. Trav. Chim. Pays−Bas* **1985**, *104*, 309. (f) Shainyan, B. A. *Usp. Khim.* **1986**, *55*, 942. (g) Rappoport, Z. *Acc. Chem. Res.* **1992**, *25*, 474.

(2) (a) Bernasconi, C. F.; Fassberg, J.; Killion, R. B., Jr.; Rappoport, Z. *J. Am. Chem. Soc.* **1989**, *111*, 6862. (b) Bernasconi, C. F.; Fassberg, J.; Killion, R. B., Jr.; Rappoport, Z. *J. Am. Chem. Soc.* **1990**, *112*, 3169. (c) Bernasconi, C. F.; Leyes, A. E.; Rappoport, Z.; Eventova, I. *J. Am. Chem. Soc.* **1993**, *115*, 7513. (d) Bernasconi, C. F.; Schuck, D. F.; Ketner, R. J.; Weiss, M.; Rappoport, Z. *J. Am. Chem. Soc.* **1994**, *116*, 11764. (e) Bernasconi, C. F.; Leyes, A. E.; Eventova, I.; Rappoport, Z. *J. Am. Chem. Soc.* **1995**, *117*, 1703. (f) Bernasconi, C. F.; Schuck, D. F.; Ketner, R. J.; Eventova, I.; Rappoport, Z. *J. Am. Chem. Soc.* **1995**, *117*, 2719.

(3) Bernasconi, C. F.; Ketner, R. J.; Chen, X.; Rappoport, Z. *J. Am. Chem. Soc.* **1998**, *120*, 7461.

(4) Bernasconi, C. F.; Ketner, R. J.; Chen, X.; Rappoport, Z. *Can. J. Chem.* **1999**, *77*, 584.

10.1021/jo991041k CCC: $18.00
Published on Web 11/26/1999

subjected to reaction with an acidic solution. This yields k_{-1}^{H} and k_2^{H}; k_1^{NuH} can be obtained as $k_1^{NuH} = K_1^{NuH}\ k_{-1}^{H}$ with K_1^{NuH} being the equilibrium constant for NuH addition and related by $K_1^{NuH} = K_1^{Nu}\ K_a^{NuH}$ to the known equilibrium constant for Nu^- addition[3,4] and the acidity constant of NuH (K_a^{NuH}). Such a study is now reported for the acid-catalyzed breakdown of alkoxide and thiolate ion adducts of **1-OMe** and **1-SMe**, as well as the corresponding adducts of benzylidene Meldrum's acid, **1-H**.[5] These latter reactions serve as reference points that allow an assessment of the effect of the methoxy in **1-OMe** and thiomethoxy groups in **1-SMe** on the reactivity of the respective systems.

Results

General Features. All kinetic experiments were performed in 50% DMSO−50% water (v/v) at 20 °C and conducted under pseudo-first-order conditions, with the substrates/adducts as the minor component. The adducts were generated in situ by reaction of a given substrate with a basic solution of the respective alkoxide or thiolate ion. In the case of **1-H**, the adducts were quite stable; with **1-OMe** and **1-SMe**, solutions of the respective adducts started to decompose within a few minutes, either as a result of conversion to substitution products or hydrolysis of the substrate[3,4] that is in equilibrium with the adduct. This made it imperative to initiate the reaction with acid immediately after the adduct had been generated. The reactions were monitored spectrophotometrically, exploiting the large differences in the UV spectra between the intermediates and the reactants or products.[3−5]

1-H. A. Alkoxide Ion Adducts. The adducts, **1-(H,OR)**$^-$ with R = H, CH_3, $HC{\equiv}CCH_2$, and CF_3CH_2, were investigated. When a solution of **1-(H,OR)**$^-$ was added

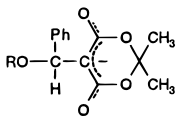

1-(H,OR)$^-$

to an HCl solution, two kinetic processes were observed. The first is associated with partial recovery of **1-H** and is quite fast. Plots of k_{obsd}^{fast} vs $[H^+]$ are shown for two cases in Figure 1; the plot for **1-(H,OMe)**$^-$ is also representative for **1-(H,OH)**$^-$, while the plot for **1-(H,OCH$_2$C≡CH)**$^-$ is also representative for **1-(H,OCH$_2$CF$_3$)**$^-$. The second, slower, process completes the recovery of **1-H**. For the reaction of **1-(H,OH)**$^-$ and **1-(H,OMe)**$^-$, k_{obsd}^{slow} is pH-independent between $[H^+] = 0.0012-0.16$ M, whereas for **1-(H,OCH$_2$C≡CH)**$^-$ and **1-(H,OCH$_2$CF$_3$)**$^-$, k_{obsd}^{slow} depends non-linearly on $[H^+]$. Figure 2 shows a representative plot.

These results can be understood on the basis of eq 3.

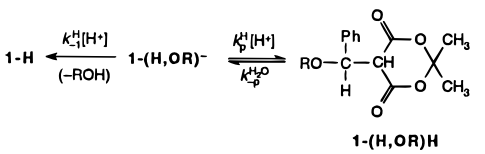

1-(H,OR)H (3)

The fast process corresponds to reaction of **1-(H,OR)**$^-$ with the hydronium ion, which leads to a mixture of **1-H** (acid-

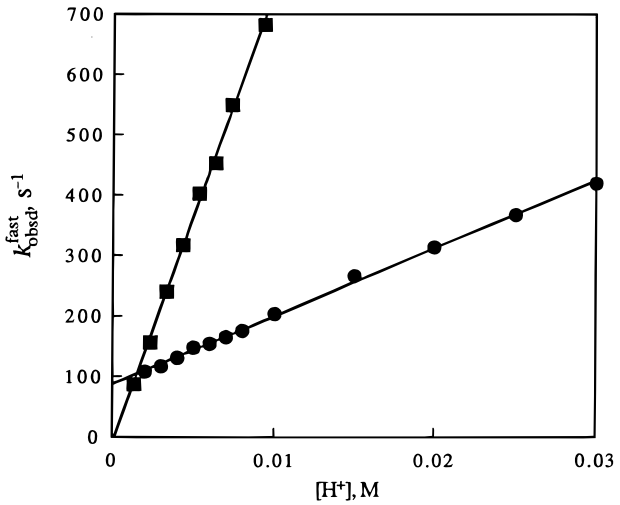

Figure 1. Reactions of **1-(H,OR)**$^-$ with HCl. Plots of k_{obsd}^{fast} vs $[H^+]$. ■, R = Me; ●, R = $HC{\equiv}CCH_2$.

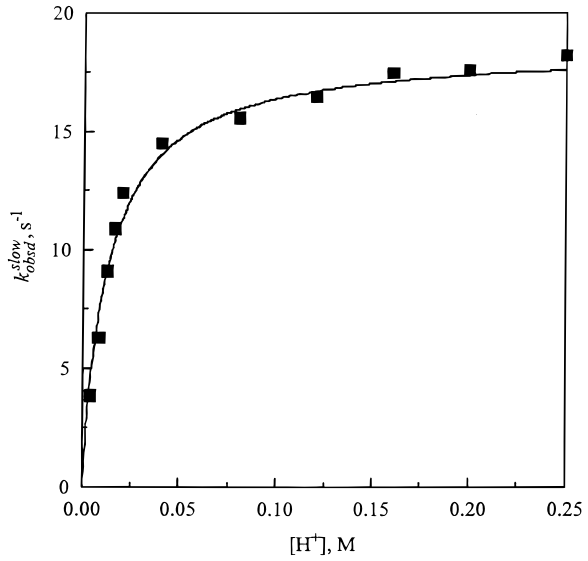

Figure 2. Reaction of **1-(H,OCH$_2$CF$_3$)** with HCl. Plot of k_{obsd}^{slow} vs $[H^+]$ according to eq 9.

catalyzed RO^- departure, $k_{-1}^{H}[H^+]$) and **1-(H,OR)H** (protonation on carbon, $k_p^{H}[H^+]$). Under conditions where $(k_{-1}^{H} + k_p^{H})[H^+] \gg k_{-p}^{H_2O}$, k_{obsd}^{fast} is given by eq 4. The very

$$k_{obsd}^{fast} = (k_{-1}^{H} + k_p^{H})[H^+] \qquad (4)$$

small intercepts in the plots of k_{obsd}^{fast} vs $[H^+]$ for the reactions of **1-(H,OMe)**$^-$ (Figure 1) and **1-(H,OH)**$^-$ (plot not shown) indicate that this condition is met over nearly the entire range of $[H^+]$. However, in the reactions of **1-(H,OCH$_2$C≡CH)**$^-$ (Figure 1) and **1-(H,OCH$_2$CF$_3$)**$^-$ (not shown), the intercepts are not negligible, indicating that the relationship $(k_{-1}^{H} + k_p^{H})[H^+] \gg k_{-p}^{H_2O}$ is not valid. In these cases the expression for k_{obsd}^{fast} becomes quite complex,[6] although the slope of these plots may still be approximated by eq 5.

$$\text{slope} \approx k_{-1}^{H} + k_p^{H} \qquad (5)$$

The individual k_{-1}^{H} and k_p^{H} values (Table 1) were obtained by combining the slopes (eq 5) with eq 6

(5) Bernasconi, C. F.; Ketner, R. J. *J. Org. Chem.* **1998**, *63*, 6266.

Table 1. Rate Constants for H^+-Catalyzed RO^- Departure from 1-(H,OR)$^-$ and Carbon Protonation of 1-(H,OR)$^-$ and pK_a^{CH} Values of 1-(H,OR)H

RO^-	pK_a^{ROH}	k_p^H [a] $M^{-1}\,s^{-1}$	$k_{-p}^{H_2O}$ [b] s^{-1}	pK_a^{CH} [d]	pK_a^{CH} [e]	k_{-1}^H [a] $M^{-1}\,s^{-1}$	k_{-1}^H [e] $M^{-1}\,s^{-1}$
HO^-	17.3	$(1.83 \pm 0.01) \times 10^4$	37.2 ± 2.4	2.69 ± 0.03		$(1.33 \pm 0.07) \times 10^5$	
MeO^-	17.2	$(1.27 \pm 0.02) \times 10^4$	50.4 ± 1.8	2.40 ± 0.03		$(6.25 \pm 0.11) \times 10^4$	
$HC{\equiv}CCH_2O^-$	15.2	$(5.46 \pm 0.08) \times 10^3$	47.0 ± 0.8[c]	2.06 ± 0.02	2.34 ± 0.04	$(5.77 \pm 0.09) \times 10^3$	$(5.57 \pm 0.39) \times 10^3$
$CF_3CH_2O^-$	14.0	$(2.63 \pm 0.12) \times 10^3$	39.9 ± 1.8[c]	1.82 ± 0.03	1.87 ± 0.04	$(2.11 \pm 0.10) \times 10^3$	$(1.40 \pm 0.09) \times 10^3$

[a] From k_{obsd}^{fast} (eqs 4 and 5 combined with eq 6). [b] From k_{obsd}^{slow} (eq 8). [c] From plateau at high $[H^+]$. [d] $pK_a^{CH} = -\log(k_{-p}^{H_2O}/k_p^H)$ with k_p^H from k_{obsd}^{fast} (eqs 4 and 5 combined with eq 6) and $k_{-p}^{H_2O}$ from k_{obsd}^{slow} (eq 8). [e] From k_{obsd}^{slow} (eq 9).

Table 2. Rate Constants for H^+-Catalyzed RS^- Departure from 1-(H,SR)$^-$ and Carbon Protonation of 1-(H,SR)$^-$ and pK_a^{CH} and pK_a^{OH} Values of 1-(H,SR)H

RS^-	pK_a^{RSH}	pK_a^{OH} [a]	pK_a^{CH} [b]	pK_a^{CH} [c]	k_p^H [a] $M^{-1}\,s^{-1}$	$k_{-p}^{H_2O}$ [d] s^{-1}	$k_{-p}^{H_2O}$ s^{-1}	k_{-1}^H [e] $M^{-1}\,s^{-1}$
n-Bu^-	11.40	1.39 ± 0.08	~2.55	2.07 ± 0.03	$(1.90 \pm 0.42) \times 10^4$	52 ± 40	162 ± 43	28.3 ± 1.0
MeS^-	≈11.0	1.27 ± 0.08	2.09 ± 0.22	2.03 ± 0.03	$(1.68 \pm 0.34) \times 10^4$	135 ± 38	156 ± 43	17.9 ± 0.8
$HOCH_2CH_2S^-$	10.56	1.11 ± 0.06	1.90 ± 0.09	1.90 ± 0.04	$(1.31 \pm 0.15) \times 10^4$	166 ± 18	165 ± 39	6.62 ± 0.99
$MeO_2CCH_2CH_2S^-$	10.40	1.13 ± 0.05	1.89 ± 0.11	1.80 ± 0.03	$(1.07 \pm 0.17) \times 10^4$	139 ± 19	168 ± 38	2.61 ± 0.10
$MeO_2CCH_2S^-$	8.83	0.99 ± 0.06	1.50 ± 0.09		$(0.93 \pm 0.13) \times 10^4$	291 ± 19	232 ± 41	0.17 ± 0.04[e]

[a] From k_{obsd}^{fast} (eq 11). [b] $pK_a^{CH} = -\log(k_{-p}^{H_2O}/k_p^H)$ with k_p^H and $k_{-p}^{H_2O}$ from k_{obsd}^{fast} (eq 11). [c] From k_{obsd}^{slow} (eq 12). [d] $k_{-p}^{H_2O} = K_a^{CH}\,k_p^H$ with K_a^{CH} from k_{obsd}^{slow} (eq 14). [e] Calculated from eq 14 with K_a^{CH} from k_{obsd}^{fast}.

Table 3. Summary of Rate Constants for Spontaneous (k_{-1}) and H^+-Catalyzed (k_{-1}^H) Breakdown of 1-(H,OR)$^-$ and 1-(H,SR)$^-$, for Nucleophilic Addition of ROH and RSH to 1-H (k_1^{NuH}), and Other Relevant Parameters

nucleophile	pK_a^{NuH}	k_{-1} [b] s^{-1}	k_{-1}^H [c] $M^{-1}\,s^{-1}$	k_{-1}^H/k_{-1} M^{-1}	pH (50)[d]	K_1^{NuH} [e]	k_1^{NuH} [f] $M^{-1}\,s^{-1}$
			1-(H,OR)$^-$				
H_2O	17.33[a]	1.57×10^{-7}	1.33×10^5	8.47×10^{11}	11.93	5.43×10^{-8} [h]	7.10×10^{-3} [i]
MeOH	17.2	2.35×10^{-6}	6.25×10^4	2.66×10^{10}	10.42	*j*	*j*
$HC{\equiv}CCH_2OH$	15.2	4.71×10^{-4}	5.67×10^3 [g]	1.20×10^7	7.08	5.26×10^{-8}	2.98×10^{-4}
CF_3CH_2OH	14.0	3.25×10^{-3}	1.75×10^3 [g]	5.38×10^5	5.73	6.43×10^{-8}	1.13×10^{-4}
			1-(H,SR)$^-$				
n-BuSH	11.40	4.25×10^{-5}	28.3	6.66×10^5	5.82	2.34	66.2
MeSH	≈11.0		17.9				
$HOCH_2CH_2SH$	10.56	2.68×10^{-4}	6.62	2.47×10^4	4.39	1.45	9.80
$MeO_2CCH_2CH_2SH$	10.40	3.21×10^{-4}	2.61	8.13×10^3	3.91	1.86	4.85
MeO_2CCH_2SH	8.83	3.35×10^{-3}	0.17	5.07×10^1	1.71	3.14	0.66

[a] Based on $pK_w = 15.89$; Hallé, J.; Gaboriaud, R.; Schaal, R. *Bull. Soc. Chim. Fr.* **1970**, 2047. [b] Reference 5. [c] This work. [d] pH for which $k_{-1}^H[H^+] = k_{-1}$. [e] $K_1^{NuH} = K_1^{Nu}\,K_a^{NuH}$ with K_1^{NuH} from ref 5. [f] $k_1^{NuH} = K_1^{NuH}\,k_{-1}^H$. [g] Average of the two values reported in Table 1. [h] Obtained by dividing observed K_1^{NuH} by $[H_2O]$. [i] Using $K_1^{NuH} = 5.43 \times 10^{-8}$ to define k_1^{NuH} as bimolecular rate constant. [j] Not experimentally measurable in 50% DMSO−50% water.

$$\frac{k_{-1}^H}{k_{-1}^H + k_p^H} = \frac{\Delta OD_{fast}}{\Delta OD_{total}} \qquad (6)$$

where ΔOD_{fast} refers to the change in absorbance associated with the fast process and ΔOD_{total} refers to the absorbance change corresponding to total recovery of **1-H**. Note that in conjunction with the known[5] equilibrium constant, K_1^{NuH}, for eq 7, k_1^{NuH} for nucleophilic attack on

$$\textbf{1-H} + ROH \overset{K_1^{NuH}}{\rightleftharpoons} \textbf{1-(H,OR)}^- + H^+ \qquad (7)$$

1-H by ROH can be obtained as $K_1^{NuH}\,k_{-1}^H$ (Table 3).

In regards to the slow process, for **1-(H,OH)**$^-$ and **1-(H,OMe)**$^-$ it represents conversion of **1-(H,OR)H** to **1-H** via **1-(H,OR)**$^-$ as a steady-state intermediate, with k_{obsd}^{slow} given by eq 8. This is consistent with the observation that k_{obsd}^{slow} is independent of $[H^+]$. Equation 8 can be solved for $k_{-p}^{H_2O}$ which is the only unknown.

$$k_{obsd}^{slow} = \frac{k_{-p}^{H_2O} k_{-1}^H}{k_p^H k_{-1}^H} \qquad (8)$$

For the $HC{\equiv}CCH_2$ and CF_3CH_2 derivatives, **1-(H,OR)**$^-$ cannot be considered a steady-state intermediate except at the high end of the $[H^+]$ range, i.e., where k_{obsd}^{slow} reaches a plateau (Figure 2). This plateau corresponds to eq 8. At low $[H^+]$ the acid−base equilibrium between **1-(H,OR)**$^-$ and **1-(H,OR)H** no longer favors **1-(H,OR)-H**. If this proton transfer is treated as a rapid equilibrium and k_{-1}^H as the rate-limiting step, we may approximate k_{obsd}^{slow} by eq 9, with $K_a^{CH} = k_{-p}^{H_2O}/k_p^H$ being the acidity

$$k_{obsd}^{slow} = \frac{K_a^{CH} k_{-1}^H [H]^+}{K_a^{CH} + [H^+]} \qquad (9)$$

constant of **1-(H,OR)H**. A least-squares curve fit of the plots of k_{obsd}^{slow} vs $[H^+]$ according to eq 9 yields k_{-1}^H and K_a^{CH}. As can be seen from the results summarized in Table 1, the k_{-1}^H values obtained from eq 9 are in good to excellent agreement with those obtained from eqs 5 and 6; there is also good agreement between the K_a^{CH} values obtained from k_{obsd}^{fast} and k_{obsd}^{slow} in the case of **1-(H,-OCH$_2$CF$_3$)H** but a somewhat larger discrepancy for the

(6) Bernasconi, C. F. *Relaxation Kinetics*; Academic Press: New York, 1976; Chapter 3.

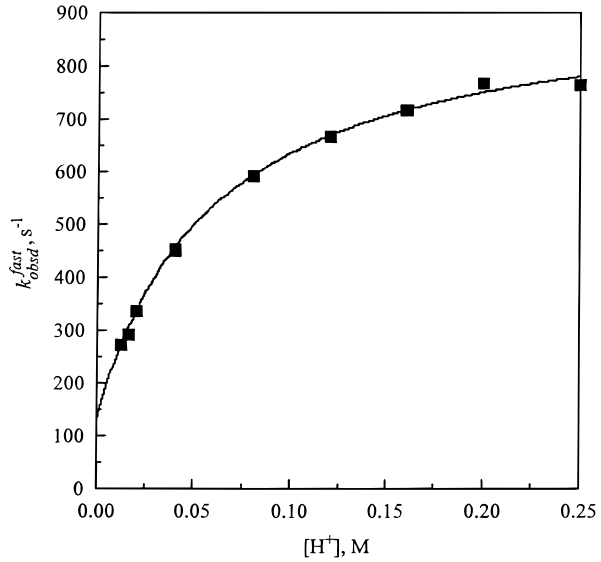

Figure 3. Reaction of **1-(H,SR)**$^-$ (R = $MeO_2CCH_2CH_2$) with HCl. Plot of k_{obsd}^{fast} vs [H^+] according to eq 11.

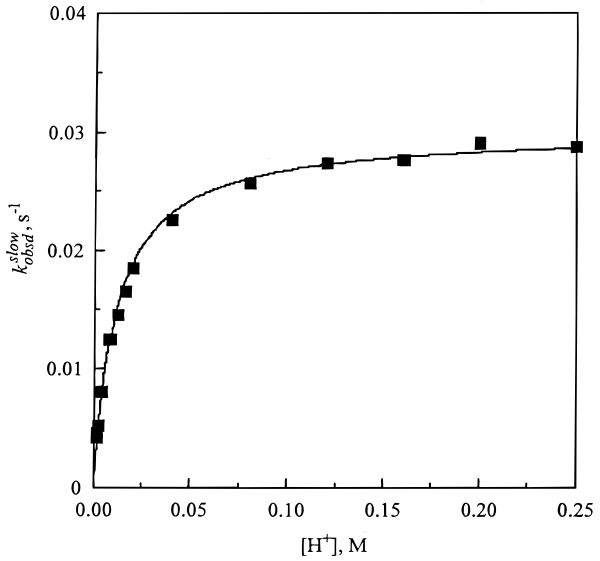

Figure 4. Reaction of **1-(H,SR)**$^-$ (R = $MeO_2CCH_2CH_2$) with HCl. Plot of k_{obsd}^{slow} vs [H^+] according to eq 12.

propargyl derivative. In view of the approximations that underlie eqs 5 and 9 in this case, though, the discrepancy is remarkably small.

B. Thiolate Ion Adducts. The adducts, **1-(H,SR)**$^-$ with R = CH_3, *n*-Bu, $HOCH_2CH_2$, $MeO_2CCH_2CH_2$, and MeO_2CCH_2, were investigated. Just as is the case for

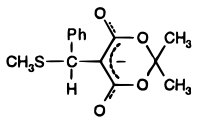

1-(H,SR)$^-$

1-(H,OR)$^-$, reaction of **1-(H,SR)**$^-$ with HCl leads to two kinetic processes. However, only the second, slower process brings about recovery of **1-H**; there is no increase in absorbance at 325 nm (λ_{max} of **1-H**) associated with the first, faster process, which simply leads to protonation of the adduct. There are also important differences in the *kinetic* results for the thiolate adducts compared to the alkoxy adducts.

Figure 3 shows a plot of k_{obsd}^{fast} vs [H^+] for the reaction of **1-(H,SCH$_2$CH$_2$CO$_2$Me)**$^-$; it is representative for the fast process with all five adducts. The second reaction is several orders of magnitude slower. Figure 4 displays a plot of k_{obsd}^{slow} vs [H^+] for the reaction of the same adduct, which is also representative for R = *n*-Bu, CH_3, $HOCH_2$-CH_2, and $MeO_2CCH_2CH_2$. With R = MeO_2CCH_2 no satisfactory data could be obtained at [HCl] < 0.1 M because the absorbance changes were too small; at [HCl] = 0.1−0.5 M k_{obsd}^{slow} *was* measurable and showed no dependence on [H^+].

We offer the following interpretation. The fast process is consistent with eq 10 where protonation occurs both

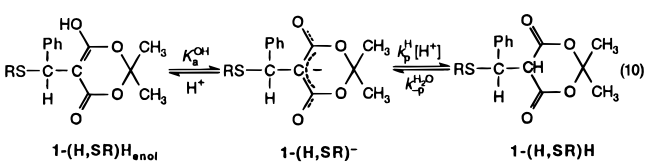

1-(H,SR)H$_{enol}$ **1-(H,SR)**$^-$ **1-(H,SR)H** (10)

on carbon and oxygen; the protonation on oxygen is too fast to be measurable on the stopped-flow time scale and acts as a rapid pre-equilibrium preceding protonation on carbon. Based on eq 10, k_{obsd}^{fast} is given by eq 11; a non-

$$k_{obsd}^{fast} = \frac{K_a^{OH} k_p^H [H^+]}{K_a^{OH} + [H^+]} + k_{-p}^{H_2O} \qquad (11)$$

linear least-squares fit yields the K_a^{OH}, k_p^H and $k_{-p}^{H_2O}$ values summarized in Table 2.

The slow process can be understood based on Scheme 1 in which both proton transfer equilibria are rapidly established on the time scale of the conversion of **1-(H,-SR)**$^-$ to **1-H**; k_{obsd}^{slow} is given by eq 12.

$$k_{obsd}^{slow} = \frac{K_a^{OH} K_a^{CH}}{K_a^{OH} K_a^{CH} + (K_a^{OH} + K_a^{CH})[H^+]} (k_{-1} + k_{-1}^H [H^+]) \qquad (12)$$

We shall first discuss the results for **1-(H,SR)**$^-$ with R = *n*-Bu, Me, $HOCH_2CH_2$, and $MeO_2CCH_2CH_2$ for which the plots of k_{obsd}^{slow} vs [H^+] are as shown in Figure 4. These plots are consistent with $k_{-1} \ll k_{-1}^H [H^+]$ which reduces eq 12 to eq 13 at low [H^+] and to eq 14

$$k_{obsd}^{slow} = k_{-1}^H [H^+] \qquad (13)$$

$$k_{obsd}^{slow} = \frac{K_a^{OH} K_a^{CH}}{K_a^{OH} + K_a^{CH}} k_{-1}^H \qquad (14)$$

at high [H^+]. The k_{-1}^H and K_a^{CH} values obtained by fitting the data to eq 14 are summarized in Table 2. For the MeS, $HOCH_2CH_2S$, and $MeO_2CCH_2CH_2S$ derivatives the K_a^{CH} values obtained from k_{obsd}^{fast} (as $pK_a^{CH} = -\log(k_{-p}^{H_2O}/k_p^H)$) and from k_{obsd}^{slow} are in remarkably good agreement. However, for the *n*-BuS derivative the agreement is poor. This is not surprising because of the very large uncertainty in the $k_{-p}^{H_2O}$ value used to calculate pK_a^{CH} in this case. For this reason $k_{-p}^{H_2O}$ calculated as $K_a^{CH} k_p^H$ with pK_a^{CH} from k_{obsd}^{slow} will be taken as the correct value for the *n*-BuS derivative.

Scheme 1

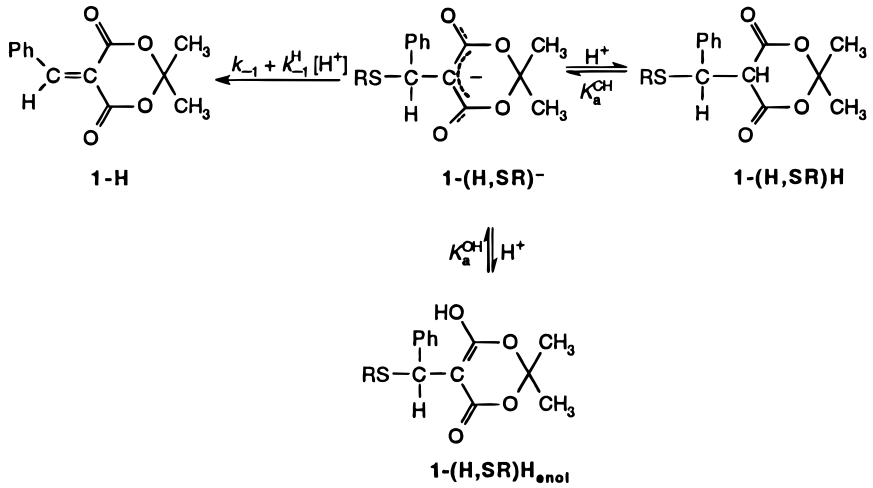

For the MeO_2CCH_2S derivative the absence of data for k_{obsd}^{slow} at low $[H^+]$ precludes a determination of pK_a^{CH} and k_{-1}^H, although it seems clear that the k_{obsd}^{slow} values at $[H^+]$ = 0.1−0.5 M are consistent with eq 14. Using pK_a^{CH} obtained from k_{obsd}^{fast}, eq 14 can be solved for k_{-1}^H as the only unknown.

Just as for the reaction of **1-(H,OR)**$^-$, the k_{-1}^H values allow calculation of $k_1^{NuH} = K_1^{NuH}\, k_{-1}^H$ (Table 3) for nucleophilic attack on **1-H** by RSH because the equilibrium constants for thiol addition, K_1^{NuH}, are known from a previous study.[5]

A referee has raised the possibility of a competing pathway which converts **1-(H,SR)H**$_{enol}$ directly into **1-H**. This would add a term to eq 12 to yield eq 15 with k'_{-1}

$$k_{obsd} = \frac{K_a^{OH}K_a^{CH}}{K_a^{OH}K_a^{CH} + (K_a^{OH} + K_a^{CH})[H^+]}(k_{-1} + k_{-1}^H[H^+]) + \frac{K_a^{CH}[H^+]}{K_a^{OH}K_a^{CH} + (K_a^{OH} + K_a^{CH})[H^+]}k'_{-1} \quad (15)$$

being the rate constant for direct conversion of **1-(H,SR)H**$_{enol}$ to **1-H**. Hence what is reported as k_{-1}^H in Table 2 would take on the meaning of $k_{-1}^H + k'_{-1}/K_a^{OH}$. For the k'_{-1} pathway to contribute equally to the reaction as the k_{-1}^H pathway, the relationship $k'_{-1} = K_a^{OH}\, k_{-1}^H$ would have to hold. Because the K_a^{OH} values are on the order of 0.05−0.1 (Table 2) this would require k'_{-1} to be not less than 5−10% of k_{-1}^H. In view of the absence of a negative charge on **1-(H,SR)H**$_{enol}$ which in **1-(H,SR)**$^-$ provides the main driving force of the reaction, such a high value for k'_{-1} seems unlikely.

1-OMe and 1-SMe. Alkoxide and Thiolate Ion Adducts. The following adducts were investigated: **1-(OMe,OR)**$^-$ with R = CH_3, $HC{\equiv}CCH_2$, and CF_3CH_2; **1-(OMe,SR)**$^-$ with R = *n*-Bu, CH_3, $HOCH_2CH_2$, $MeO_2CCH_2CH_2$, and MeO_2CCH_2; and **1-(SMe,SMe)**$^-$. The

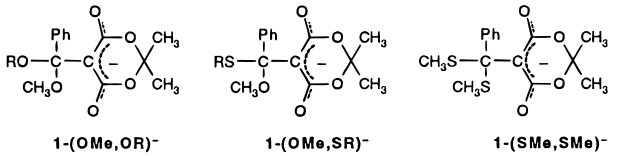

Scheme 2

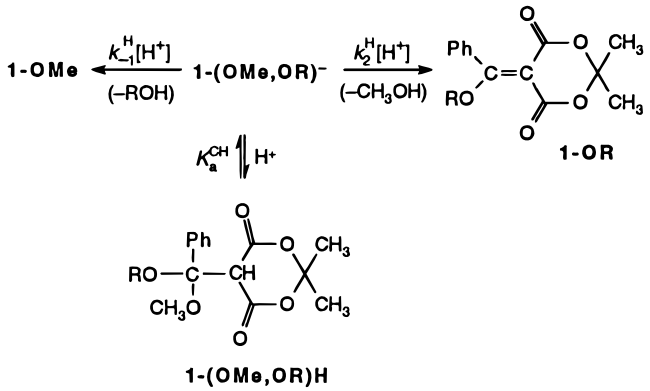

Scheme 3

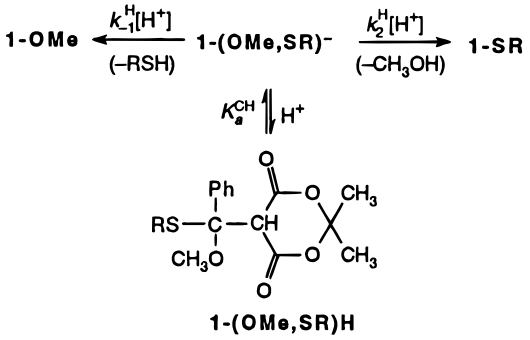

quenching of any of these adducts with HCl generated one fast kinetic process followed by one or two much slower reactions. The slow processes were shown to represent the previously reported[3,4] hydrolysis of the respective products of the fast process, i.e., **1-OMe**, **1-OR**, or **1-SR** (see Schemes 2−4).

For the fast process, plots of k_{obsd}^{fast} vs $[H^+]$ are curved in most cases, as shown in Figure 5 for two representative examples. This observation is consistent with concurrent H^+-catalyzed loss of both leaving groups from the respective intermediate; protonation on carbon acts as a fast pre-equilibrium, which is the cause of the downward curvature in the plots (Figure 5). This is shown in Schemes 2, 3, and 4, respectively, for the various cases.

Note that in Scheme 4 a statistical factor of 2 is

Scheme 4

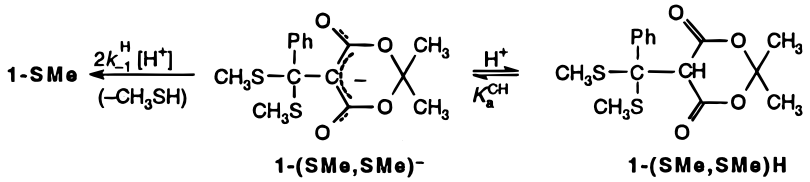

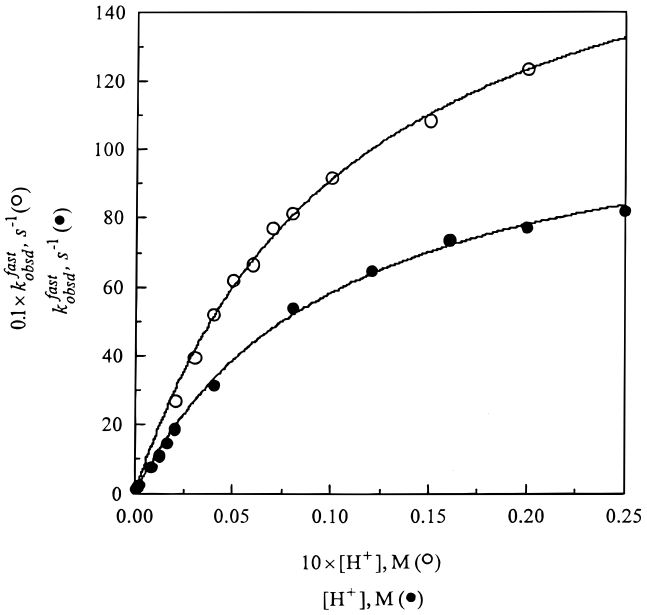

Figure 5. Reactions of **1-(OMe,OMe)**$^-$ (○) and **1-(SMe,SMe)**$^-$ (●) with HCl. Plots of k_{obsd}^{fast} vs [H$^+$] according to eq 15 (**1-(OMe,OMe)**$^-$) or eq 16 (**1-(SMe,SMe)**$^-$).

included to render the k_{-1}^{H} value comparable to k_{-1}^{H} in Scheme 3 when making structure−reactivity comparisons.

The expression for k_{obsd}^{fast} for Schemes 2 and 3 is given by eq 15, and for Scheme 4 it is given by eq 16.

$$k_{obsd}^{fast} = \frac{K_a^{CH}}{K_a^{CH} + [H^+]}(k_{-1}^{H} + k_2^{H})[H^+] \qquad (15)$$

$$k_{obsd}^{fast} = 2\,\frac{K_a^{CH}}{K_a^{CH} + [H^+]}k_{-1}^{H}[H^+] \qquad (16)$$

Non-linear least-squares fit of the data to eqs 15 and 16 yielded $k_{-1}^{H} + k_2^{H}$ (Schemes 2 and 3) and k_{-1}^{H} (Scheme 4), respectively. In cases where curvature is strong, a value for K_a^{CH} was also obtained; in situations where the curvature is weak, no K_a^{CH} values are reported because of large experimental uncertainty.

In the reactions described by Scheme 3 the spectra of the solutions at the end of the reaction showed that the main species formed was **1-SR** (λ_{max} = 335 nm[4,7]), with smaller amounts of **1-OMe** (λ_{max} = 272 nm).[3] This implies $k_2^{H} > k_{-1}^{H}$. Because of considerable overlap of the spectra of **1-SR** and **1-OMe**, no precise k_2^{H}/k_{-1}^{H} ratio could be determined from an analysis of these spectra. However, k_2^{H}/k_{-1}^{H} ratios were obtained by exploiting the fact that **1-OMe** hydrolyzes much more rapidly ($t_{1/2} \approx$ 23 s)[3] than **1-SR** ($t_{1/2} \approx$ 68.7 h).[4,8] The change in absorbance at 270 nm that resulted from this hydrolysis provided a measure of the amount of **1-OMe** that had been generated in the reaction of **1-(OMe,SR)**$^-$ with HCl. This allowed a determination of the k_2^{H}/k_{-1}^{H} ratios and in conjunction with $k_{-1}^{H} + k_2^{H}$ afforded k_{-1}^{H} and k_2^{H} individually (Table 4). The large experimental uncertainty associated with the k_{-1}^{H} values is the result of the rather small amounts of **1-OMe** formed in the reaction.

For the reactions shown in Scheme 2 with R ≠ CH$_3$ the above methodology could not be used to determine k_{-1}^{H} and k_2^{H} individually. HPLC analysis, which was successfully applied for such purpose in the reactions of acid with alkoxide ion adducts of β-methoxy-α-nitrostilbene,[2f] could not be used here either because the hydrolysis of **1-OR** and **1-OMe** is too fast ($t_{1/2}$ = 23 s for **1-OMe** and shorter for **1-OR**). However, for the case R = CH$_3$, $k_{-1}^{H} = k_2^{H}$ could be obtained just as is the case for the reaction of Scheme 4.

A few selected experiments were also conducted in acetate buffers ranging in pH from 4.7 to 6.8. The adducts subjected to this study were of the type **1-(OMe,SR)**$^-$ with R = *n*-Bu, MeO$_2$CCH$_2$CH$_2$, and MeO$_2$CCH$_2$. Buffer catalysis was weak at [AcOH] ≤ 0.04 M and typically amounted to less than 7% increase in k_{obsd} at the highest concentration.

Discussion

Mechanism of Acid Catalysis. Acid catalysis of alkoxide ion departure from addition complexes between electrophiles and alkoxide or hydroxide ions has frequently been observed.[2b,9−11] These reactions are typically subject to general acid catalysis. The weak catalysis of MeO$^-$ departure from **1-(OMe,SR)**$^-$ by acetic acid and results reported previously for the reactions of **1-(H,OR)**$^-$ (R = HC≡CCH$_2$ and CF$_3$CH$_2$) with Et$_3$NH$^+$ [5] also indicate general acid catalysis. This kind of catalysis has generally been interpreted in terms of a concerted mechanism[12] with a transition state such as **2** shown for the breakdown of **1-(H,OR)**$^-$ catalyzed by a buffer acid BH$^{\nu+1}$ and **3** for H$_3$O$^+$ as the catalyst.[14] Evidence presented below

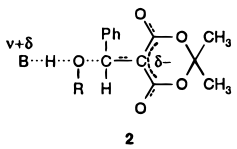

2

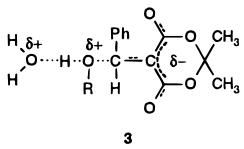

3

(7) λ_{max} is virtually independent of the R group.

(8) $t_{1/2} \approx$ 68.7 h refers to the hydrolysis of **1-SMe**.

(9) Jencks, W. P. *Chem. Rev.* **1985**, *85*, 511 and numerous references therein.

(10) (a) Bernasconi, C. F. *Tetrahedron* **1989**, *45*, 4017 and numerous references therein. (b) Bernasconi, C. F.; Fassberg, J. *J. Am. Chem. Soc.* **1994**, *116*, 514.

(11) Bernasconi, C. F.; Fassberg, J.; Killion, R. B., Jr.; Schuck, D. F.; Rappoport, Z. *J. Am. Chem. Soc.* **1991**, *113*, 4937.

(12) This mechanism is usually referred to as a class n mechanism.[13]

(13) Jencks, W. P. *Chem. Soc. Rev.* **1981**, *10*, 345.

Table 4. Rate Constants for H^+-Catalyzed RO^- and RS^- Departure from Various Adducts and pK_a^{CH} Values of Some Adducts

adduct	pK_a^{NuH}	$k_{-1}^H + k_2^H$ $M^{-1}\,s^{-1}$	k_{-1}^H $M^{-1}\,s^{-1}$	k_2^H $M^{-1}\,s^{-1}$	pK_a^{CH}
1-(OMe,OMe)$^-$	17.2[a]	$(1.77 \pm 0.05) \times 10^5$	$(8.85 \pm 0.25) \times 10^4$ (−MeOH)		1.97 ± 0.03
1-(OMe,OCH$_2$C≡CH)$^-$	15.2[a]	$(3.02 \pm 0.08) \times 10^4$			1.78 ± 0.02
1-(OMe,OCH$_2$CF$_3$)$^-$	14.0[a]	$(4.02 \pm 0.40) \times 10^3$			
1-(OMe,SBu)$^-$	11.40[b]	$(1.97 \pm 0.40) \times 10^5$	$(2.7 \pm 0.8) \times 10^4$ (−BuSH)	$(1.70 \pm 0.48) \times 10^5$ (−MeOH)	
1-(OMe,SMe)$^-$	≈11.0[b]	$(7.55 \pm 0.10) \times 10^4$	$(8.9 \pm 2.0) \times 10^3$ (−MeSH)	$(7.00 \pm 0.30) \times 10^4$ (−MeOH)	1.18 ± 0.10
1-(OMe,SCH$_2$CH$_2$OH)$^-$	10.56[b]	$(3.39 \pm 0.10) \times 10^4$	$(5.9 \pm 1.1) \times 10^3$ (−HOCH$_2$CH$_2$SH)	$(2.80 \pm 0.26) \times 10^4$ (−MeOH)	
1-(OMe,SCH$_2$CH$_2$CO$_2$Me)$^-$	10.40[b]	$(2.81 \pm 0.45) \times 10^4$			
1-(OMe,SCH$_2$CO$_2$Me)$^-$	8.83[b]	$(6.83 \pm 1.31) \times 10^3$	$(2.2 \pm 0.7) \times 10^3$ (−MeO$_2$CCH$_2$SH)	$(4.6 \pm 2.0) \times 10^3$ (−MeOH)	
1-(SMe,SMe)$^-$	≈11.0[b]	$(1.16 \pm 0.04) \times 10^3$	$(5.80 \pm 0.20) \times 10^2$ (−MeSH)		

[a] NuH = ROH. [b] NuH = RSH.

Table 5. Summary of Rate Constants for Spontaneous (k_{-1}) and H^+-Catalyzed (k_{-1}^H and k_2^H) Breakdown of 1-(OMe,OMe)$^-$ and 1-(OMe,SR)$^-$, for Nucleophilic Addition of MeOH and RSH to 1-OMe (k_1^{NuH}), and Other Relevant Parameters

Nu	pK_a^{NuH}	k_{-1}[a] s^{-1}	k_{-1}^H $M^{-1}\,s^{-1}$	k_{-1}^H/k_{-1} M^{-1}	pH (50)[c]	K_1^{NuH}[d]
MeOH	17.2	6.1×10^{-6}[g]	8.85×10^4[g]	1.45×10^{10}	10.2	
n-BuSH	11.40	0.395	2.7×10^4	6.84×10^4	4.83	6.77×10^{-7}
HOCH$_2$CH$_2$SH	10.56	1.71	5.9×10^3	3.45×10^3	3.54	7.08×10^{-7}
MeO$_2$CCH$_2$SH	8.83	14.0	2.2×10^3	1.57×10^2	2.20	2.53×10^{-6}

Nu	k_1^{NuH}[e] $M^{-1}\,s^{-1}$	k_2[a] s^{-1}	k_2^H[b] $M^{-1}\,s^{-1}$	k_2^H/k_2 M^{-1}	pH (50)[f]
n-BuSH	1.83×10^{-2}	1.11×10^{-4}	1.7×10^5	1.5×10^9	9.18
HOCH$_2$CH$_2$SH	4.18×10^{-3}	2.16×10^{-4}	2.8×10^4	1.3×10^8	8.11
MeO$_2$CCH$_2$SH	5.57×10^{-3}		4.6×10^3		

[a] Reference 3. [b] This work. [c] pH for which $k_{-1}^H[H^+] = k_{-1}$. [d] $K_1^{NuH} = K_1^{Nu}\,K_a^{NuH}$ with K_1^{Nu} from ref 3. [e] $k_1^{NuH} = K_1^{NuH}\,k_{-1}^H$. [f] pH for which $k_2^H[H^+] = k_2$. [g] Statistically corrected.

suggests that, at least for **3**, proton transfer to the RO group is more advanced than C−O bond cleavage, as represented by the position of the transferred proton and the placement of a partial positive charge on the RO oxygen in **3**. Note that by virtue of the principle of microscopic reversibility, **2** and **3** are also the transition states for general base-catalyzed and water-catalyzed, respectively, nucleophilic attack by the neutral alcohol.

Acid catalysis of thiolate ion departure or its microscopic reverse, addition of thiols, has not been reported as often. Examples include the reactions of PhS^-/PhSH with 1-chloro-2,4,6-trinitrobenzene in methanol−water mixtures[15] and with 7-halogeno-4-nitrobenzofurazan[16] in methanol and the reactions of $HOCH_2CH_2S^-$/$HOCH_2CH_2$-SH with the tri-*p*-anisylmethyl cation in water.[17] It is likely that the mechanism is the same as for the alcohol reactions.

The reason why acid catalysis of thiolate ion departure or its microscopic reverse has not been reported as frequently as for alkoxide ion or OH^- expulsions is related to the narrower pH range within which such catalysis can be detected. This pH range is determined by the k_{-1}^H/k_{-1} ratios, with k_{-1} referring to spontaneous loss of the leaving group. The acid-catalyzed process contributes 50% to the overall rate when $k_{-1}^H[H^+]/k_{-1} = 1$. From the k_{-1}^H/k_{-1} ratios summarized in Table 3 (**1-(H,OR)$^-$** and **1-(H,SR)$^-$**) and Table 5 (**1-(OMe,SR)$^-$**) we can deduce that acid catalysis contributes 50% to the rate at much higher pH values for alkoxide than for thiolate ion loss ("pH(50)" columns in Tables 3 and 5).[18] Hence, unless experiments are conducted at rather low pH, acid catalysis remains undetected. The lower k_{-1}^H/k_{-1} ratios for thiolate ion departure are the combined result of a lower sensitivity to acid catalysis due to the lower proton basicity of thiolate compared to alkoxide ions and the higher rate constants for spontaneous loss (k_{-1}) of thiolate compared to alkoxide ions.

Kinetic and Thermodynamic Stabilities of 1-(OMe,SR)$^-$ vs 1-(H,SR)$^-$ and of 1-(OMe,OMe)$^-$ vs 1-(H,OMe)$^-$. The k_{-1}^H values for the H^+-catalyzed loss of thiolate ions are substantially larger for **1-(OMe,SR)$^-$** (Table 5) than for **1-(H,SR)$^-$** (Table 3), with k_{-1}^H(**1-OMe,SR**)$^-$/k_{-1}^H(**1-H,SR**)$^-$ ratios ranging from ca. 10^3 to 10^4. This largely reflects the much smaller equilibrium constants, K_1^{NuH}, for RSH addition to **1-OMe** (Table 5) compared to **1-H** (Table 3), with K_1^{NuH}(**1-OMe**)/

(14) As pointed out by a referee, the H_3O^+-catalyzed reaction could alternatively be stepwise, involving pre-equilibrium protonation of the leaving group by H_3O^+ followed by carbon-heavy atom bond cleavage. We prefer the concerted mechanism (**3**) because of its similarity to the mechanism of buffer catalysis.

(15) Forlani, L. *J. Chem. Res. (S)* **1992**, 376.

(16) de Rosso, M. D.; Di Nunno, L.; Florio, S.; Amorese, A. *J. Chem. Soc., Perkin Trans. 2* **1980**, 239.

(17) Ritchie, C. D.; Gandler, J. R. *J. Am. Chem. Soc.* **1979**, *101*, 7318.

(18) A similar approach to this problem has been discussed by Jensen and Jencks[19] for the acid-catalyzed hydrolysis of benzaldehyde *O,S*-acetals. We are indebted to a referee for pointing this out.

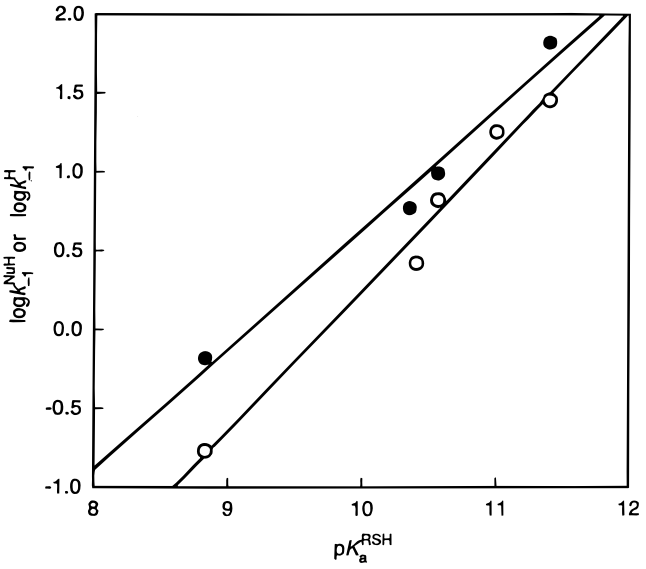

Figure 6. Brønsted plots for the reaction **1-H** + RSH ⇄ **1-(H,-SR)**$^-$ + H$^+$. ●, k_1^{NuH} (NuH = RSH); ○, k_{-1}^{H}.

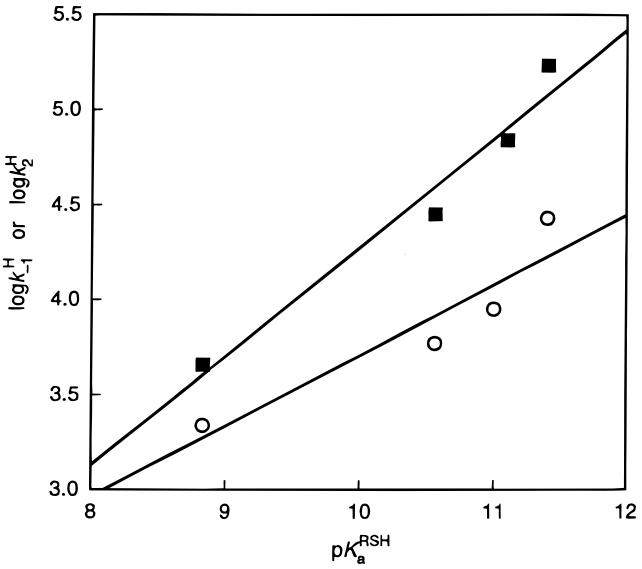

Figure 7. Brønsted plots for the reactions **1-OMe** + RSH ← **1-(OMe,SR)**$^-$ + H$^+$ → **1-SR** + MeOH. ○, k_{-1}^{H}; ■, k_2^{H}.

K_1^{NuH}(**1-H**) ratios ranging from ca. 3×10^{-7} to 8×10^{-7}.[20] The main reasons for the much smaller equilibrium constants for **1-OMe** are the greater steric crowding in the adduct and the ground-state stabilization of **1-OMe** by the π-donor effect of the methoxy group, as discussed in more detail elsewhere.[3,4]

For **1-(OMe,OMe)**$^-$ the k_{-1}^{H} value (8.85×10^4 M^{-1} s^{-1}, Table 5) is very nearly the same as $k_{-1}^{H} = 6.25 \times 10^4$ M^{-1} s^{-1} for **1-(H,OMe)**$^-$ (Table 3). This is consistent with the equilibrium constants, K_1^{NuH}, for MeOH addition to **1-OMe** (K_1^{NuH} = ca. 1.7×10^{-9}, Table 5)[21] being much less depressed compared to K_1^{NuH} for MeOH addition to **1-H** (K_1^{NuH} = ca. 5×10^{-8}, Table 3)[22] than is the case in the reactions with thiols. As discussed in detail elsewhere,[3] the relatively high equilibrium constants for the addition of oxygen nucleophiles to **1-OMe** is in large measure the result of anomeric stabilization of the adduct by the geminal alkoxy groups.[23,24]

Brønsted Coefficients. Figures 6 and 7 show some representative Brønsted plots, and Table 6 gives a summary of all Brønsted β values determined in this study, including some previously determined ones for the reactions of RO$^-$ and RS$^-$. The fact that all β_{lg} values for acid-catalyzed leaving group departure (k_{-1}^{H}) are positive indicates a transition state which, relative to the adduct, is destabilized by electron-withdrawing R groups. This implies a buildup of positive charge on the leaving-group atom, which must be the result of a transition-state imbalance[9,25,26] where proton transfer from H_3O^+ to the departing group has made more progress than C−O or C−S bond cleavage (see **3**).

Table 6. Brønsted Coefficients

parameter	1-H	1-OMe
ROH as Nucleophiles		
β_{nuc} = d log k_1^{NuH}/dpK_a^{ROH}	ca. 0.35[a,b]	
β_{lg} = d log k_{-1}^{H}/dpK_a^{ROH}	0.46 ± 0.04[a]	
"β" = d log($k_{-1}^{H} + k_2^{H}$)/dpK_a^{ROH}		0.50 ± 0.09[a]
RO$^-$ as Nucleophiles		
β_{nuc} = d log k_1^{Nu}/dpK_a^{ROH}	ca. 0.23[c]	0.51[d]
β_{lg} = d log k_{-1}/dpK_a^{ROH}	ca. −0.81[c]	−0.97[d]
RSH as Nucleophiles		
β_{nuc} = d log k_1^{NuH}/dpK_a^{RSH}	0.75 ± 0.11[a]	ca. 0.7[a]
β_{lg} = d log k_{-1}^{H}/dpK_a^{RSH}	0.85 ± 0.07[a]	0.35 ± 0.13[a]
β_{push} = d log k_2^{H}/dpK_a^{RSH}		0.58 ± 0.14[a]
RS$^-$ as Nucleophiles		
β_{nuc} = d log k_1^{Nu}/dpK_a^{RSH}	0.17[c]	0.17[d]
β_{lg} = d log k_{-1}/dpK_a^{RSH}	−0.72[c]	−0.59[d]
β_{push} = d log k_2/dpK_a^{RSH}		0.75[d]

[a] This study. [b] Based on two points only. [c] Reference 5. [d] Reference 3.

In the direction of nucleophilic attack by ROH or RSH (k_1^{NuH}), the β_{nuc} values are also positive, just as β_{lg} for k_{-1}^{H}, consistent with transition state **3** which, relative to the reactants, is being destabilized by electron-withdrawing R groups. Incidentally, a consequence of both β_{lg} and β_{nuc} being positive is that K_1^{NuH} depends little on the R group.

The positive β_{lg} values for acid-catalyzed leaving-group expulsion contrast with the negative β_{lg} values for *spontaneous* departure of RO$^-$ and RS$^-$ (k_{-1}). These latter values reflect the buildup of negative charge on the leaving-group atom at the transition state (**4**, X = O or S). In the direction of nucleophilic attack by RO$^-$ or RS$^-$

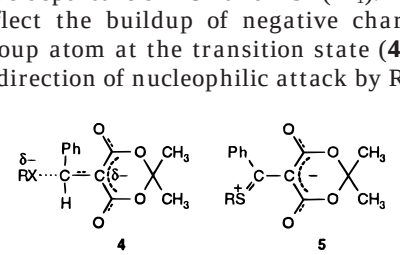

4 **5**

(19) Jensen, J. L.; Jencks, W. P. *J. Am. Chem. Soc.* **1979**, *101*, 1476.

(20) Note that the K_1^{NuH}(**1-OMe**)/K_1^{NuH}(**1-H**) ratios are the same as the K_1^{Nu}(**1-OMe**)/K_1^{Nu}(**1-H**) ratios because $K_1^{NuH} = K_1^{Nu}$ K_w.

(21) K_1^{NuH} for **1-(OMe,OMe)**$^-$ estimated as the average of K_1^{NuH} for **1-(OMe,OCH$_2$C≡CH)**$^-$ and **1-(OMe,OCH$_2$CH$_3$)**$^-$.

(22) K_1^{NuH} for **1-(H,OMe)**$^-$ estimated as the average of K_1^{NuH} for **1-(H,OR)**$^-$ with R = H, HC≡CCH$_2$, and CF$_3$CH$_2$.

(23) (a) Kirby, A. G. *The Anomeric Effect and Related Stereoelectronic Effects of Oxygen*; Springer−Verlag: Berlin, 1983. (b) Schleyer, P. v. R.; Jemmis, E. D.; Spitznagel, G. W. *J. Am. Chem. Soc.* **1985**, *107*, 6393.

(24) (a) Hine, J.; Klueppl, A. W. *J. Am. Chem. Soc.* **1974**, *96*, 2924. (b) Wiberg, K. B.; Squires, R. R. *J. Chem. Thermodyn.* **1979**, *11*, 773. (c) Harcourt, M. P.; More O'Ferrall, R. A. *Bull. Soc. Chim. Fr.* **1988**, 407.

Table 7. Rate Constants for the Spontaneous (k_{-1}, k_2) and H^+-Catalyzed (k^H_{-1}, k^H_2) Collapse of RO^- Adducts of β-Alkoxy-α-nitrostilbenes[a,b]

	6-$(OCH_2CF_3)_2^-$		**6-(OMe,OCH_2CF_3)$^-$**		**6-$(OMe)_2^-$**
k_{-1}, s^{-1}	8.25×10^{-6} [c] ($-CF_3CH_2O^-$)	$\beta_{push} = 0.24$	5.0×10^{-5} ($-CF_3CH_2O^-$)	$\beta_{lg} = -1.06$	2.0×10^{-8} [c] ($-CH_3O^-$)
k_2, s^{-1}		$\beta_{lg} = -0.82$	$<2.0 \times 10^{-8}$ ($-CH_3O^-$)	$\beta_{push} > 0$	
k^H_{-1}, $M^{-1}\ s^{-1}$	0.40[c] ($-CF_3CH_2OH$)	$\beta_{push} = 0.66$	51.9 ($-CF_3CH_2OH$)	$\beta_{lg} = 0.26$	3.73×10^{2} [c] ($-CH_3OH$)
k^H_2, $M^{-1}\ s^{-1}$		$\beta_{lg} = 0.35$	5.42 ($-CH_3OH$)	$\beta_{push} = 0.57$	
k^H_{-1}/k_{-1}, M^{-1}	4.85×10^4		1.40×10^6		1.86×10^{10}
k^H_2/k_2, M^{-1}			$>1.36 \times 10^8$		

[a] In 50% Me_2SO−50% water at 20 °C (μ = 0.5 M KCl); ref 2f. [b] The various β_{push} and β_{lg} values were obtained from comparisons of pairs of rate constants. For example, $\beta_{push} = 0.24$ refers to a comparison of k_{-1} for the loss of $CF_3CH_2O^-$ from **6-$(OCH_2CF_3)_2^-$** with that from **6-(OMe,OCH_2CF_3)$^-$**, i.e., it is a measure of the increased push by the MeO group compared to the CF_3CH_2O group. [c] Statistically corrected.

(k_1^{Nu}) the β_{nuc} values are "normal," i.e., positive, a consequence of partial loss of the negative charge on RX^- when entering the transition state.

Table 6 reports a β_{push} value (0.58) for the H^+-catalyzed MeO^- loss from **1-(OMe,SR)$^-$**. This value comes from a plot of log k_2^H vs pK_a^{RSH}, i.e., it is the group left behind that is varied while the leaving group is constant. The positive value of β_{push} is the result of an electronic push by the π-donor effect of the RS group, which leads to resonance stabilization in the incipient product (**5**).

For the reaction of the **1-(OMe,OR)$^-$** adducts (R ≠ Me) only the sum of k^H_{-1} and k^H_2 and not the individual rate constants could be determined. A plot of $\log(k^H_{-1} + k^H_2)$ vs pK_a^{ROH} (not shown) yields a slope "β" = 0.50 ± 0.09 (Table 6). This is a reasonable value because k^H_{-1} is expected to decrease with decreasing pK_a^{ROH} (positive β_{lg}) as is the case for ROH departure from **1-(H,OR)$^-$** (β_{lg} = 0.46) and k_2^H is also expected to decrease with decreasing pK_a^{ROH} (positive β_{push}), as in the case of MeOH departure from **1-(OMe,SR)$^-$** (β_{push} = 0.58).

pK_a^{CH} Values. The pK_a^{CH} values of the **1-(H,OR)H** complexes range from 1.82 to 2.69 (Table 1), for the **1-(H,SR)H** complexes from 1.80 to 2.07, for the **1-(OMe,OR)H** complexes from 1.78 to 1.97 (Table 4), while the pK_a^{CH} of **1-(OMe,SMe)** is 1.18 (Table 4). These pK_a^{CH} values are considerably lower than the pK_a^{CH} of Meldrum's acid (4.70),[27] indicating that the electron-withdrawing effect of the PhCH(OR), PhCH(SR), PhC(OMe)OR, and PhC(OMe)SMe moieties is substantial, and apparently reflect stabilization of the carbanion. The trend toward lower pK_a^{CH} values with decreasing pK_a^{NuH} of the nucleophile is a manifestation of the same phenomenon.

It is noteworthy that the pK_a^{CH} values for the alkoxide and thiolate ion complexes derived from **1-H** are quite similar to each other or even slightly lower for the thiolate ion adducts, despite the stronger electron-withdrawing inductive/field effect of RO compared to RS groups.[28] The stronger acidifying effect of a thio group compared to an alkoxy group is even more apparent when comparing the pK_a^{CH} values of **1-(OMe,SMe)H** (1.18) with those of **1-(OMe,OMe)H** (1.97) and **1-(OMe,-$OCH_2C{\equiv}CH$)H** (1.78). This is probably the result of the greater polarizability of the sulfur compared to the oxygen substituents. Sulfur substituents on the α-carbon of carbanions are known to exert a strong stabilizing effect;[30,31] our results suggest that even in the β-position there is still a modest stabilizing effect.

Comparisons with RO^- Adducts of β-Alkoxy-α-nitrostilbenes. It is instructive to compare the rate constants for the collapse of **1-(OMe,OR)$^-$** with the corresponding rate constants for the collapse of similar adducts derived from β-alkoxy-α-nitrostilbenes, specifically, **6-$(OMe)_2^-$**, **6-(OMe,OCH_2CF_3)$^-$**, and **6-$(OCH_2CF_3)_2^-$**.[2f] They are summarized in Table 7.

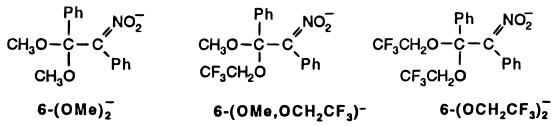

The following points are noteworthy. (1) The k^H_{-1}/k_{-1} ratio of 1.45×10^{10} M^{-1} for **1-$(OMe)_2^-$** is about the same as for **6-$(OMe)_2^-$** (1.86×10^{10} M^{-1}), but the absolute values of k_{-1} and k^H_{-1} for **1-$(OMe)_2^-$** are more than 200-fold higher than for **6-$(OMe)_2^-$**. As pointed out elsewhere,[2f] the fact that the absolute values of k_{-1} are higher for **1-$(OMe)_2^-$** than for **6-$(OMe)_2^-$** is particularly remarkable because **1-$(OMe)_2^-$** is thermodynamically more favored relative to its precursor (**1-OMe**) than **6-$(OMe)_2^-$** relative to β-methoxy-α-nitrostilbene. The rea-

(25) Jencks, D. A.; Jencks, W. P. *J. Am. Chem. Soc.* **1977**, *99*, 7948.
(26) Bernasconi, C. F. *Acc. Chem. Res.* **1987**, *20*, 301. (b) Bernasconi, C. F. *Acc. Chem. Res.* **1992**, *25*, 9. (c) Bernasconi, C. F. *Adv. Phys. Org. Chem.* **1992**, *27*, 119.
(27) Bernasconi, C. F.; Oliphant, N., unpublished results.
(28) The σ_F values for MeO and MeS are 0.30 and 0.20, respectively.[29]
(29) Hansch, C.; Leo, A.; Taft, R. W. *Chem. Rev.* **1991**, *91*, 165.
(30) For reviews, see (a) Price, C. C.; Oae, S. *Sulfur Bonding*; Ronald Press: New York, 1962. (b) Cram, D. J. *Fundamentals of Carbanion Chemistry*; Academic Press: New York, 1965; pp 71−84. (c) Eliel, E. L.; Hartmann, A. A.; Abatjoglou, A. G. *J. Am. Chem. Soc.* **1974**, *96*, 1807. (d) Bordwell, F. G.; Bares, J. E.; Bartmess, J. E.; Drucker, G. F.; Gerhold, J.; McCollum, G. J.; Van der Puy, M.; Vanier, N. R.; Matthews, W. S. *J. Org. Chem.* **1977**, *42*, 326.
(31) Bernasconi, C. F.; Kittredge, K. W. *J. Org. Chem.* **1998**, *63*, 1944.

son for the higher kinetic reactivity of **1-(OMe)$_2^-$** is that the *intrinsic* rate constant[32] is higher. This is because resonance plays a lesser role[26] in the stabilization of **1-(OMe)$_2^-$** and similar adducts derived from Meldrum's acid than in the case of **6-(OMe)$_2^-$** and analogues. (2) The β_{lg} and β_{push} values based on two-point comparisons reported in Table 7 follow the same qualitative patterns seen for the Meldrum's acid derivatives. In particular, the β_{lg} values for spontaneous loss of RO^- are large negative numbers (-0.97 for **1-OMe** vs -0.82 and -1.06 for the nitrostilbene derivatives) but positive for H^+-catalyzed RO^- loss ("β" = 0.50 for **1-OMe** vs 0.35 and 0.26 for the nitrostilbene derivatives), while β_{push} is positive in all cases. Apparently, the *relative* reactivities governed by the change of leaving groups (β_{lg}) or groups that are left behind (β_{push}) are not affected in a major way by the changes in the intrinsic rate constants.

Proton-Transfer Rate Constants. Rate constants for the proton-transfer reactions of eq 17 are summarized

$$\textbf{1-(H,XR)}^- + H_3O^+ \underset{k_{-p}^{H_2O}}{\overset{k_p^H}{\rightleftharpoons}} \textbf{1-(H,XR)H} + H_2O \quad (17)$$

in Table 2 for X = O and Table 3 for X = S. Some of these rate constants are subject to a relatively large experimental uncertainty. For example, this can be seen from the large standard deviations for $k_{-p}^{H_2O}$ in the reaction of **1-(H,SR)H** and the fact that two methods of determining these $k_{-p}^{H_2O}$ values yield different values. In the case of **1-(H,OR)**, the $k_{-p}^{H_2O}$ values may be subject to systematic errors that are much larger than the standard deviations. This is because they were obtained by solving eq 8, which contains two rate constants that may have their own systematic errors. This may explain why $k_{-p}^{H_2O}$ for the alkoxide ion adducts does not show the expected trend toward lower values with increasing pK_a^{CH}.

For these reasons and also because the pK_a^{CH} ranges are quite small, one cannot expect to obtain meaningful Brønsted coefficients for these reactions and none are reported. The same is true for the *intrinsic* rate constants, (k_0),[32] that are usually determined by suitable extrapolation of the Brønsted plots.[26] Nevertheless, the fact that for a given pK_a^{CH}, both k_p^H and $k_{-p}^{H_2O}$ are about 3- to 4-fold higher for the sulfur compared to the oxygen compounds indicates that the intrinsic rate constant for the sulfur complexes is higher than that for the oxygen complexes by a similar factor.

The higher intrinsic rate constants for the sulfur complexes may be attributed to the same polarizability effect that is responsible for the acidity of **1-(H,SR)H** that is higher than what is expected on the basis of the inductive/field effect of the RS group. As discussed in much more detail elsewhere,[31] an enhancement of the intrinsic rate constant will occur if the stabilization of the transition state by the polarizability effect is disproportionately strong relative to that of the fully developed carbanion **1-(H,SR)**$^-$. This is likely to be the case, because in the deprotonation of carbon acids that lead to resonance-delocalized carbanions, the delocalization has typically made little progress at the transition state.[26] This implies that the negative charge is mainly localized on the α-carbon, as indicated in exaggerated form in **7**.

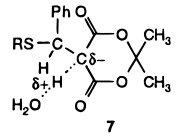

7

Hence the stabilization of this charge resulting from the polarizability of the sulfur is relatively more effective than the stabilization of the more remote delocalized charge in the carbanions.[33]

It should be noted that the enhancement of the intrinsic rate constant for the thiolate ion adducts relative to the alkoxide ion adducts of **1-H** is rather modest because the RS groups are one carbon removed from the α-carbon. In cases where the RS group is on the α-carbon, the effect is considerably larger.[31]

pK_a^{OH} of 1-(H,SR)H$_{enol}$. In strongly acidic solution, rapid protonation of one of the carbonyl oxygens of **1-(H,SR)**$^-$ or **1-(H,OR)**$^-$ to form an enol (eq 10), acts as a pre-equilibrium step that precedes protonation on carbon (k_p^H) and acid-catalyzed RS^- expulsion (k_{-1}^H). In the case of **1-(H,SR)** the pK_a^{OH} of the enol could be determined because the plot of k_{obsd}^{fast} vs [H^+] levels off (pH < pK_a^{OH}) before k_{obsd}^{fast} becomes too large for stopped-flow measurements (Figure 5). For **1-(H,OR)**$^-$ no such leveling could be observed within the limits of the stopped-flow technique, and hence pK_a^{OH} was inaccessible.

The pK_a^{OH} values of **1-(H,SR)H$_{enol}$** are about 0.7−0.8 log units lower than the pK_a^{CH} values (Table 3) and show a similar dependence on pK_a^{RSH} of the thiol as the pK_a^{CH} values. In comparison, the pK_a^{OH} value of the enol form of Meldrum's acid (2.48)[35,36] is 2.35 log units lower than the pK_a^{CH} (4.83).[35,36] The smaller difference between pK_a^{OH} and pK_a^{CH} implies that the enolization equilibrium constants, which are given by eq 18, are larger for **1-(H,SR)H** (0.15−0.20) than for Meldrum's acid (4.47×10^{-3}).[35,36] This indicates a stabilization of the enol and/or a destabilization of the ester form by the PhCH(SR) substituent. Our results are consistent with reports that the enolization constants of β-diketones are generally enhanced by electron-withdrawing substituents on the α-carbon,[37] an enhancement that has been attributed to a destabilization of the keto form due to increased positive charge on the carbonyl carbons.[37]

$$K_E = \frac{[\text{enol}]}{[\text{ester}]} = \frac{K_a^{CH}}{K_a^{OH}} \quad (18)$$

Conclusions

(1) Thiolate ion departure is much less sensitive to H^+-catalysis than alkoxide ion departure, as reflected in much smaller k_{-1}^H/k_{-1} and k_2^H/k_2 ratios for the former. This is the result of the lower basicity of the thiolate ions,

(32) For a reaction with a forward rate constants k_f and a reverse rate constant k_r the intrinsic rate constants, k_0, is defined as $k_0 = k_f = k_r$ when $K = k_f / k_r = 1$ ($\Delta G_0 = 0$).

(33) This is true for the inductive/field effect as well, but the degree to which the transition state benefits more from the polarizability factor relative to the carbanion is larger because the polarizability effect falls off more rapidly with distance than does the inductive/field effect.[34]

(34) Taft, R. W.; Topsom, R. D. *Prog. Phys. Org. Chem.* **1987**, *16*, 1.
(35) Eigen, M.; Ilgenfritz, G.; Kruse, W. *Chem. Ber.* **1965**, *98*, 1623.
(36) In water at 25 °C.
(37) Toullec, J. In *The Chemistry of Enols*; Rappoport, Z., Ed.; Wiley & Sons: New York, 1990; p 323.

which leads to reduced acid catalysis (k_{-1}^{H}, k_2^{H}) but enhanced spontaneous departure (k_{-1}, k_2).

(2) H^+-catalyzed loss of RS^- from **1-(OMe,SR)**$^-$ is much faster than from **1-(H,SR)**$^-$, reflecting the larger thermodynamic driving force (smaller K_1^{NuH}) for expulsion of thiolate ion from **1-(OMe,SR)**$^-$ compared to **1-(H,SR)**$^-$. The H^+-catalyzed loss of MeO^- from **1-(OMe,OMe)**$^-$ is about the same as for loss from **1-(H,OMe)**$^-$, reflecting comparable thermodynamic driving forces, i.e., similar K_1^{NuH} values.

(3) The β_{lg} values for H^+-catalyzed RO^- or RS^- departure are positive and imply an imbalanced transition state where proton transfer from H_3O^+ to the departing group is ahead of C−O or C−S bond cleavage. The positive β_{push} values are the result of an electronic push by the π-donor effect of the group left behind, which leads to resonance stabilization in the incipient product.

(4) The β_{lg} and β_{push} values are comparable to those found earlier for the nitrostilbene systems. However, the absolute rate constants for adduct collapse of the Meldrum's acid derivatives are higher than those for the nitrostilbene derivatives because of the diminished role played by resonance effects in the adducts, which leads to higher intrinsic rate constants.

(5) The pK_a^{CH} values of the various adducts are much lower than the pK_a^{CH} of Meldrum's acid, indicating that the negative charge in the adducts is stabilized by the PhCH(OR), PhCH(SR), PhC(OMe)OR, and PhC(OMe)SMe groups. The effect is stronger with RS-containing groups, suggesting that the polarizability of sulfur contributes to the stabilization of the negative charge. The higher proton-transfer rate constants for the sulfur-containing adducts can also be attributed to the polarizability effect of sulfur.

(6) The enol content of **1-(H,SR)H** is significantly higher than that of Meldrum's acid, consistent with known trends according to which enolization constants of β-diketones are generally enhanced by electron-withdrawing substituents on the α-carbon.

Experimental Section

Materials. Benzylidene Meldrum's acid (**1-H**), methoxybenzylidene Meldrum's acid (**1-OMe**), and thiomethoxybenzylidene Meldrum's acid (**1-SMe**) were available from previous studies.[3−5] DMSO was refluxed over CaH_2, distilled under vacuum, and stored under dry argon. All other organic reagents, salts, and solvents were purchased from Aldrich or Fischer Chemicals. The thiols were distilled prior to use, and β-mercaptoethanol was distilled under vacuum. 2,2,2-Trifluoroethanol and propargyl alcohol were distilled and stored under nitrogen or argon. Methanol, glacial acetic acid, and KCl were used as received. Standardized solutions of HCl and KOH were prepared from Baker "Dilut-its." Millipore water was used for all experiments.

In Situ Generation of the Anionic Adducts. Solutions of the desired adduct of **1-OMe**, **1-SMe**, or **1-H** were prepared by adding microliter amounts of the substrates to a methanol solution containing the buffered nucleophile. KOMe was used as the base in preparing the nucleophile buffer. Microliter amounts of the adduct-containing solutions were then added to 50% DMSO−50% water solutions, which were used in stopped-flow experiments. The final amount of methanol was typically <1% of the solvent. Solutions of the adduct had a limited lifetime and had to be freshly prepared before each experiment.

Reaction Solutions, pH Measurements, and Kinetic Experiments. The procedures described before[3,5] were followed. All kinetic determinations were made in an Applied Photophysics DX.17MV stopped-flow apparatus.

Acknowledgment. This research was supported by Grants CHE-9307659 and CHE-9734822 from the National Science Foundation (C.F.B.) and a grant from the U.S.−Israel Binational Science Foundation, Jerusalem (Z.R.).

JO991041K